

## ANALYSIS OF FACTORS AFFECTING GRAVITY-INDUCED DEFLECTION FOR LARGE AND THIN WAFERS IN FLATNESS MEASUREMENT USING THREE-POINT-SUPPORT METHOD

Haijun Liu, Zhigang Dong, Renke Kang, Ping Zhou, Shang Gao

Dalian University of Technology, Key Laboratory for Precision and Non-Traditional Machining of Ministry of Education, 2 Linggong Road, Dalian 116024, P.R. China (liuhaijunhz@163.com, ✉ dongzg@dlut.edu.cn, +86 411 8470 7430, kangrk@dlut.edu.cn, pzhou@dlut.edu.cn, gaoshangf@gmail.com)

### Abstract

Accurate flatness measurement of silicon wafers is affected greatly by the *gravity-induced deflection* (GID) of the wafers, especially for large and thin wafers. The three-point-support method is a preferred method for the measurement, in which the GID uniquely determined by the positions of the supports could be calculated and subtracted. The accurate calculation of GID is affected by the initial stress of the wafer and the positioning errors of the supports. In this paper, a *finite element model* (FEM) including the effect of initial stress was developed to calculate GID. The influence of the initial stress of the wafer on GID calculation was investigated and verified by experiment. A systematic study of the effects of positioning errors of the support ball and the wafer on GID calculation was conducted. The results showed that the effect of the initial stress could not be neglected for ground wafers. The wafer positioning error and the circumferential error of the support were the most influential factors while the effect of the vertical positioning error was negligible in GID calculation.

Keywords: flatness measurement, large and thin silicon wafer, GID, three-point-support method, initial stress.

© 2015 Polish Academy of Sciences. All rights reserved

### 1. Introduction

With the development of 3D packaging technology, silicon wafer processing in the semiconductor manufacturing industry is getting more challenging due to reduced wafer thickness for form factor and thermal power dissipation considerations [1–4]. Wafers with low deformation are required since significant deformation caused in the thinning process results in handling and processing issues [5, 6]. The flatness measurement plays an important role in production engineering to determine if the flatness of the wafer satisfies given requirements as wafers with large deformation tend to break. Also, the flatness measurement is used for monitoring thermal and mechanical effects on the wafer shape during the wafer processing [7, 8]. However, the accurate flatness measurement of wafer is affected greatly by gravity, especially for large and thin wafers. Therefore, the *gravity-induced deflection* (GID) has to be considered in the flatness measurement of large and thin wafers.

To eliminate the effect of GID in the flatness measurement, Chu *et al.* proposed a method to obtain the shape of wafers with an interferometer while the tested wafer was floated on the surface of the high density aqueous meta-tungstate solutions [9, 10]. The front surface of the wafer was above the liquid level and the flatness was measured directly by an interferometer while the gravity was balanced by the buoyancy force. The method works well on the wafer with the total flatness error being less than its thickness, but is not suitable for the wafers with the deformation being larger than its thickness. *The Semiconductor Equipment & Materials International* (SEMI) proposed a shape measuring method [7], in which the wafer was

supported at the wafer center by a small chuck. The front surface was firstly scanned by a non-contact sensor. The wafer was then flipped over for the measurement of the back surface. The true flatness of the wafer was obtained by subtracting the two results from the corresponding measurement points. Similar to the one-point-support method, Natsu *et al.* [11] proposed a three-point-support inverting method. The wafer was supported by three rigid balls and the repeatability and the anti-disturbance ability of the flatness measurement were improved greatly in comparison with one-point-support method [12].

Both one-point-support inverting method and three-point-support inverting method work on the assumption that the effects of gravity before and after the flip of the wafer are the same during the two measurements. However, the presence of initial stresses which are caused by wafer machining in silicon wafer could have a substantial effect on its GID [13]. For double-sided polished wafers, the assumption could be valid because the damage layer is removed by polishing [14] and the initial stress is very small. For wafers after grinding or lapping, the subsurface damage is much larger and the effect of the initial stress is greater. Large errors could be introduced in the inverting method because the GIDs before and after the flip are no longer the same for silicon wafers with different initial stress states of two surfaces.

The GID of a silicon wafer could be calculated using an FEM in the three-point-support method. The unconstrained wafer shape is obtained by subtracting the GID from the measurement result. It is time-saving, since the wafer is not required to be flipped and only one measurement is needed in the flatness measurement. In this case a high precision FEM is essential for the method since it influences the flatness of the wafer directly. In the previous FEMs [15], the effect of initial stress was not taken into consideration.

Besides, the difference of positions of supports and wafer between those in the measuring experiment and in FEM will result in measurement errors. There have been few studies on systematic and quantitative evaluation of the influence of the positioning errors of the support balls on the measurement results in the three-point-support method. The positioning accuracy requirements of the supports have to be acknowledged to make the method applicable to engineering.

The objective of this paper is to provide answers to the following questions. How does the initial stress on the wafer surface affect the GID of wafers? How to obtain the FEM including the effect of initial stress under the condition that the actual initial stress value is not known? How do the positioning errors of the supports and the wafer affect the GID of wafers?

In this study, an FEM including the effect of initial stress for calculating GID of silicon wafers with the aid of the Stoney equation was developed. The simulation result of the GID of a double-sided polished wafer was compared with that measured in the experiment. A silicon wafer of which one surface was ground and the other surface was polished was measured to verify the effect of the initial stress. The effects of the positioning errors of the supporting balls and the wafer on the measurement results were examined. The error distributions on the wafer surface were studied to better understand how the measurement results were affected by the positioning errors.

## 2. Measurement principle and numerical method

A schematic of the three-point-support method is shown in Fig. 1, in which the wafer is supported at three points positioned every 120 degrees on a circle concentric with the center of the wafer. The radius of the supporting circle is defined as  $R_s$ , while the center of the wafer is located at the origin of the coordinate system.

The three-point-support method is based on the concept of superposition of multiple deflections. The surface shape of the wafer supported by three balls,  $s(x, y)$ , can be measured by a displacement sensor. As the GID of the wafer,  $g(x, y)$ , can be calculated using an FEM,

the unconstrained shape of the wafer,  $w(x, y)$ , can be obtained by subtracting the GID from the measured surface shape. The relationship between them is expressed by (1).

$$w(x, y) = s(x, y) - g(x, y). \quad (1)$$

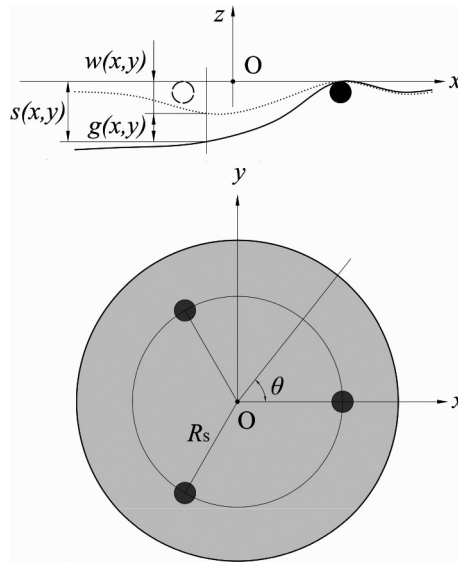


Fig. 1. An illustration of a silicon wafer supported by three balls.

An FEM including the wafer and the supporting system was used to calculate the GID of a wafer supported by three rigid balls. The wafer was meshed into quadrilateral-shaped elements for enhanced computational accuracy. The wafer-ball interface was modeled using contact elements to represent the contact and sliding between the supporting ball surfaces and the deformable wafer surface. The supporting balls were treated as rigid objects since the deformation of the balls was negligible compared with the wafer deformation. The wafer was free to move and rotate in the model. The six degrees of freedom of the supporting balls were constrained as the balls were fixed in the actual measurement scenario. The commercial software ANSYS was used in the calculations.

The wafer was supposed to consist of two layers: a bulk silicon layer and a homogeneous damage layer. For double-sided polished wafers the damage could be neglected [14]. For wafers after grinding or lapping, the residual stress on the wafer surface caused by machining was applied to the damage layer in the FEM (See Section 4). The wafer was assumed to have a uniform thickness as the thickness deviation was considerably small compared to the wafer deformation. Monocrystalline silicon is anisotropic and when the coordinate axis is parallel to the crystal orientation [100], the stiffness constants are  $c_{11} = 165.6$  GPa,  $c_{12} = 63.9$  GPa and  $c_{44} = 79.5$  GPa [16]. The mass density of silicon is  $2329 \text{ Kg/m}^3$ . The gravitational acceleration is  $9.8 \text{ m/s}^2$ . The friction coefficient between the silicon wafer and the steel ball was set at 0.2. The GID was kept re-calculated with the mesh density being doubled until the calculated results were getting to be steady and the change of the GID was less than  $0.1 \text{ }\mu\text{m}$ .

### 3. Experimental verification of FEM

An apparatus for flatness measurement was developed, consisting of a precision granite stage with aerostatic guides and grating scales in the x and y directions, a laser displacement

sensor, a supporting mechanism with three balls fixed at the bottom, and a data acquisition system, as shown in Fig. 2. Beside contact sensors [17], contactless laser sensors are often used to measure surface profiles [18]. A contactless laser displacement sensor (LK-H022K, Keyence, Japan) was adopted and mounted on the granite guide, which could move along the aerostatic guides driven by AC servo motors in the directions of x and y axes. The straightness of each guide is  $1\ \mu\text{m}$  over the full length of 500 mm. The servo motors are controlled by a Ressaix motion control system (DMC2410B, Leadshine, China). The grating scale for positioning the laser sensor has a resolution of  $0.1\ \mu\text{m}$ . The sensor could be manually moved along the z-axis, which enables adjustment of the measuring height. During measurement, the sensor moves along the x and y axes to scan a maximum area of  $500 \times 500\ \text{mm}^2$ . An application software (developed using Visual C++) is used to control the sensor's scanning path. During measurement, the positions of the sensor in the x–y plane and their corresponding value along the z-axis are recorded for calculating the wafer shape.

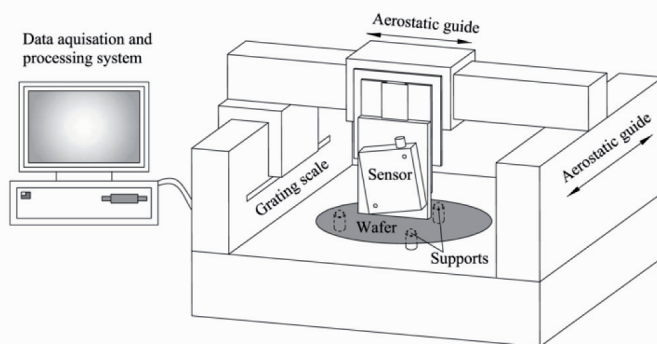


Fig. 2. A schematic illustration of the flatness measurement apparatus.

A double-sided polished single crystal (100) silicon wafer with thickness of  $330\ \mu\text{m}$  and diameter of 200 mm, provided by GRINM Advanced Materials Co. Ltd of China, was used in the verifying experiments. The surface roughness of both sides of the “as received” wafer is  $Ra\ 0.41\ \text{nm}$  measured by a white light interferometer (NewView 5022, Zygo, USA).

To verify the FEM, the simulation result of the GID of the wafer was compared with that obtained using the three-point-support inverting method in the developed apparatus shown in Fig. 2. The shape of the wafer which was supported by three balls was firstly measured along specified paths. The wafer was then turned upside down and supported by three balls at the same positions on the back side of the wafer, and the shape of the wafer was measured again [11]. The sensor moved in the x and y directions along aerostatic guides to scan the wafer while the wafer was kept static on the supporting balls during the measurement to prevent vibration. The wafer shape and the GID were obtained by processing the two measurement results at the corresponding points. The GID of the wafer under the same conditions was calculated using the developed FEM, and compared with the measured results in the experiment.

The unconstrained shape of the wafer obtained using the three-point-support inverting method is shown in Fig. 3a. The wafer has a shape showing the central symmetry and the deformation range (difference between maximum and minimum values) is about  $10\ \mu\text{m}$ . The GID distribution obtained using the three-point-support inverting method shown in Fig. 3b presents the threefold rotational symmetry which is correlated with the locations of the supporting balls. The deformation range is about  $45\ \mu\text{m}$ . The GID distribution calculated using the FEM is shown in Fig. 4, which is almost the same as the measured topography shown in Fig. 3b. The difference between the calculated and measured GIDs is presented in Fig. 5. The difference distribution does not present the threefold rotational symmetry

any more, indicating that the difference is independent from the positions of the supporting balls. The maximum difference value is about  $1.3\ \mu\text{m}$ . This difference includes the thickness variation of the wafer, since the wafer was assumed to have uniform thickness in the three-point-support inverting method [15]. The difference also includes the sensor error and the error of guide straightness. Comparing the maximum difference with the total deformation, the FEM is reliable and the error is less than 3%. The experimental results match very well the simulated values, which confirms the validity of the developed FEM.

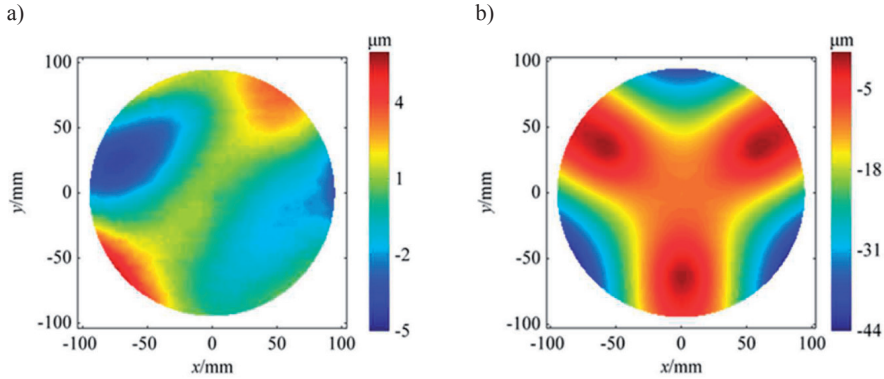


Fig. 3. a) Deformation of a double-sided polished silicon wafer; b) the GID of a silicon wafer obtained using the three-point-support inverting method.

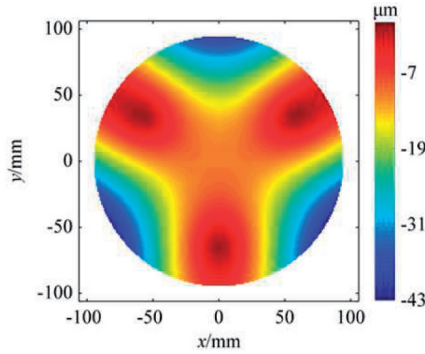


Fig. 4. The GID of a silicon wafer obtained using the FEM.

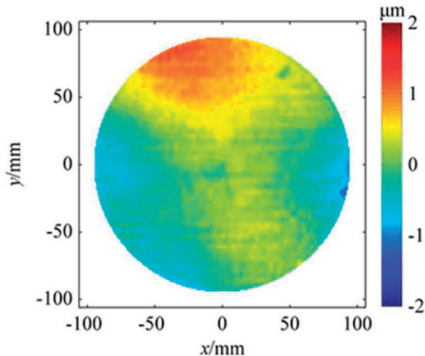


Fig. 5. The difference of GIDs presented in Fig. 4 and Fig. 3b.

#### 4. Effect of initial stress of wafer

A subsurface damage layer will be formed on the top of a crystalline silicon wafer by lapping or grinding [19–23]. For double-sided polished silicon wafers, the effect of initial stress of wafer is negligible since the subsurface damage is removed by polishing [14] and the deformation caused by the residual stress is very small, as shown in Fig. 3a. For wafers after grinding, the subsurface damage is too large to be negligible, and the wafers usually deform into a spherical cap shape due to the residual stress induced by the subsurface damage. In this study, the subsurface damage layer induced by machining is assumed to be uniform on the whole wafer surface, which has been proven to be reasonable for the wafers ground with spark-out processes [24].

A wafer of which the two surfaces were under different initial stress states was used to examine the effect of initial stress using FEMs. One surface was under a large initial stress state to mimic the ground surface whereas the other surface was stress-free to mimic the polished surface. The wafer had a diameter of 300 mm and thickness of 400  $\mu\text{m}$ . The PV value caused by the initial stress was set to be 300  $\mu\text{m}$ , which was close to that in the experiment. The GID without considering the effect of initial stress (Model A) and the GIDs considering the effect of initial stress when the ground surface was upward (Model B) and downward (Model C) were all calculated. The GID ranges, which are defined as the differences between the maximum and the minimum values, of the three models and their difference distributions are shown in Fig. 6.

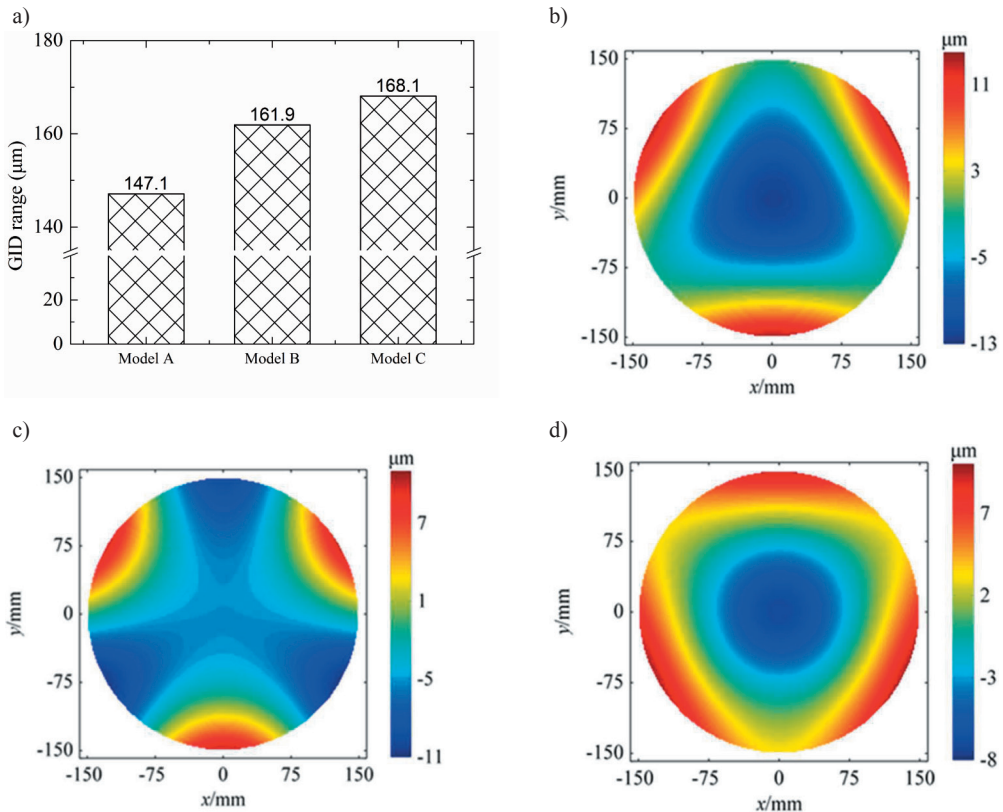


Fig. 6. Comparison of GIDs obtained by different models: a) the GID ranges of different models; b) the difference distribution between GIDs in Model A and Model B; c) the difference distribution between GIDs in Model A and Model C; d) The difference distribution between GIDs in Model B and Model C.

The GID range considering an initial stress increased by about 10% compared with that considering no initial stress, indicating the significant effect of the initial stress, as shown in Fig. 6a. Figs. 6b and 6c detail the effects of initial stress when the ground surface is upward or downward. The maximum difference values are all over 10  $\mu\text{m}$  while the GID range without considering an initial stress is 147.1  $\mu\text{m}$ . The GID obtained when the ground surface was upward also differed from that when the ground surface was downward. As shown in Fig. 6d, the maximum difference value on the wafer surface reaches 9.8  $\mu\text{m}$ , although the GID range difference is only about 6  $\mu\text{m}$ . It demonstrates the application limitation of the three-point-support inverting method which works on the assumption that the effects of gravity in two directions before and after flipping are equal.

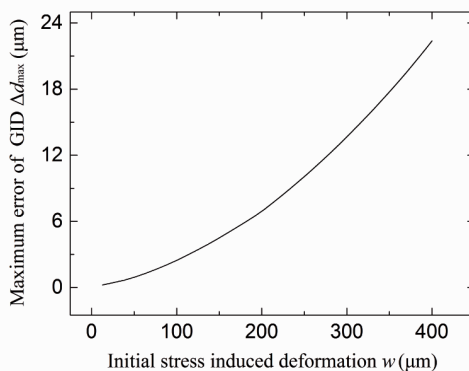


Fig. 7. The effect of an initial stress on GID.

The effect of different initial stresses on GID calculation was examined. The maximum difference value on the whole wafer surface  $\Delta d_{\text{max}}$  increases from 0 to 22.4  $\mu\text{m}$  as the initial stress induced deformation increases from 0 to 400  $\mu\text{m}$  when the ground surface was upward (Fig. 7). The slope increases with the increase of initial stress induced deformation, indicating that the effect becomes greater. In our study, the wafer was ground with #5000 diamond grinding wheel of which the grit size was about 2  $\mu\text{m}$  and the deformation was near 300  $\mu\text{m}$ . Therefore, the effect of the initial stress would be greater on wafers ground by grinding wheels with larger grit sizes, e.g. #600 or #2000 diamond grinding wheels.

In the FEM, the initial stress of the wafer is applied as a load in the wafer model when the value and the depth of the initial stress are known. However, both the value and the depth of the actual initial stress layer are not known for a certain wafer to be tested. To solve this problem, the Stoney equation was used to determine the relations between the curvature of the silicon wafer and the stress of the damage layer as the depth of the damage layer is considerably small compared with the thickness of the wafer in this study. The curvature of the machined wafer is determined by the damage induced force per unit width which bends the bulk wafer. The force per unit width along the radial direction is the integral of the stress in the film over the thickness of the film [25]. The width direction corresponds to the circumferential direction which is perpendicular to the radial direction. Therefore, the effect of the initial stress on the wafer GID could be included in the FEM after the force per unit width is calculated. The actual depth of the subsurface damage does not need to be known.

In the experiment, a silicon wafer of 300 mm diameter and 400  $\mu\text{m}$  thickness, ground by #5000 diamond grinding wheel, provided by Jing Ji Electronic Tech Co. Ltd of China, was used. The procedures of including the effect of the initial stress in the FEM are as follows:

- a) Measure the shape of the silicon wafer supported by three balls.
- b) Compute the GID of wafer using the FEM without considering the effect of initial stress.

- c) Subtract the GID from the measured result to obtain the unconstrained shape of the wafer. The calculated unconstrained shape of the wafer includes the errors caused by the initial stress of the wafer.
- d) Calculate the force per unit width of the wafer using the Stoney equation from the fitted curvature of the shape of the wafer.
- e) Compute the GID of the silicon wafer using the FEM in which the force per unit width of the wafer is applied as a load.
- f) Subtract the GID from the measured result to obtain a more accurate shape of the wafer.

In the procedure (d), the force per unit width calculation of the wafer contains errors resulted from the erroneous shape of the wafer. Besides, the procedure requires the use of a correction factor for the force per unit width calculation in the FEM under large deformation cases because the Stoney equation is based on the assumption that the strains and rotations of the wafer are infinitesimal [26]. Iterative calculation is needed to obtain the accurate shape of the wafer in the FEM. The convergence of the iterative calculation could be achieved very easily since the error of the shape is a second order small quantity in the FEM. An error of 10  $\mu\text{m}$  of 300  $\mu\text{m}$  initial stress induced deformation causes less than 1  $\mu\text{m}$  error for the GID calculation.

To verify the validity of the models, the results were compared with those obtained using the three-point-support inverting method proposed by Natsu *et al.* [11]. The GID obtained using the three-point-support inverting method was compared with the GID averaged over two directions in the FEMs as the effects of gravity in two directions were not equal.

Figures 8a and 8b detail the shape and the GID of the wafer obtained using the three-point-support inverting method. The shape of the silicon wafer is obviously a spherical one with the peak-to-valley value of about 285  $\mu\text{m}$ .

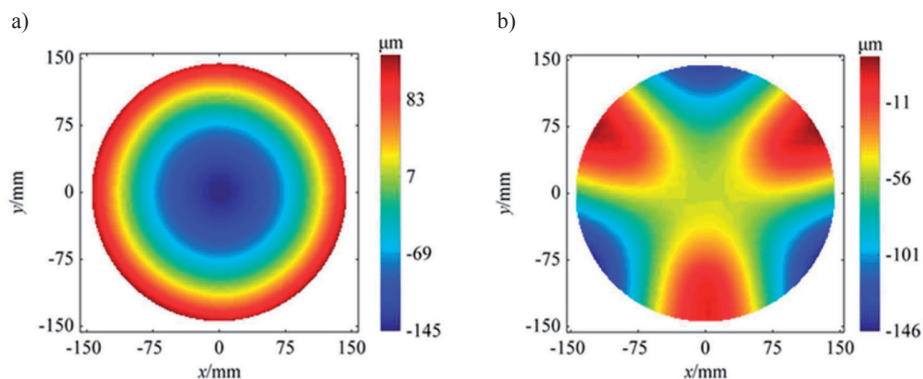


Fig. 8. a) Deformation of the ground silicon wafer; b) the GID of the wafer obtained using the three-point-support inverting method.

The GID distribution obtained by the FEM simulation without considering an initial stress, and its difference from Fig. 8b are shown in Fig. 9a and Fig. 9b. The difference distribution presents obvious correlation with the positions of the supporting balls. The maximum positive and negative difference values are over 10  $\mu\text{m}$ .

The GID distribution obtained by the FEM simulation considering an initial stress, and its difference from Fig. 8b are shown in Fig. 9c and Fig. 9d. The difference distribution indicates its independence from the positions of the supporting balls. The difference range is about half of that of Fig. 9b and the maximum difference value is about 7  $\mu\text{m}$ . Most of the difference values are less than 3  $\mu\text{m}$ . It proved that the effect of the initial stress could not be neglected.

The thickness variation of the wafer was included in the difference between the calculated and the measured topographies since the wafer was assumed to have uniform thickness

in the three-point-support inverting method [15]. The difference also included the sensor error and the error of guide straightness. When the diameter was larger, the total thickness variation increased and the sensor error and the guide straightness error both deteriorated with the increase of the scanning area.

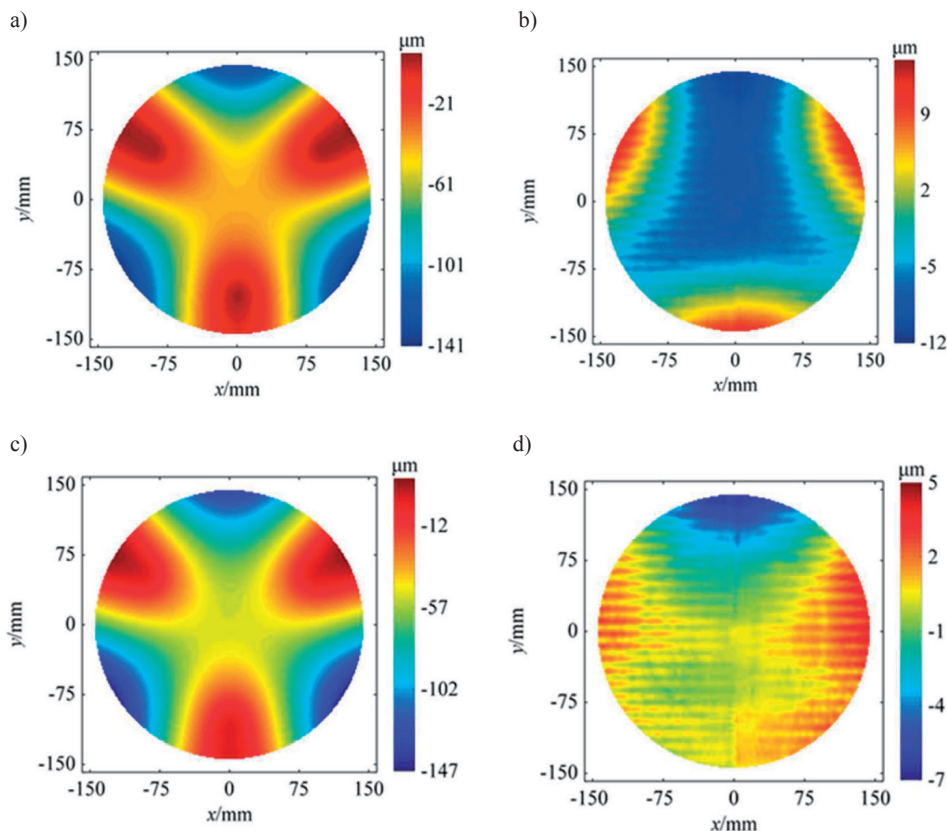


Fig. 9. a) The GID of the wafer obtained using the FEM without considering the effect of initial stress; b) difference of GIDs between those in Fig. 9a and Fig. 8b; c) the GID of the wafer obtained using the FEM considering the effect of initial stress; d) difference of GIDs between those in Fig. 9c and Fig. 8b.

### 5. Effects of positioning errors of support and wafer on GID

The positions of the supports and the wafer in the actual measuring scenario different from those in the FEM result in GID calculation errors. The GIDs of a wafer with 300 mm diameter and 400 μm thickness under different positioning errors were calculated to investigate the positioning accuracy requirements. The radius of the supporting circle  $R_s$  was set to 98 mm to minimize the GID range of the wafer.

The positioning errors of a supporting ball along the radial, circumferential and vertical directions are defined as  $e_{rd}$ ,  $e_{cd}$  and  $e_{vd}$ , respectively. The positioning error of the wafer relative to the center of the supporting circle determined by three balls is defined as  $e_{wd}$ . The difference between the GIDs with and without positioning error is defined as  $\Delta d$ , and the maximum value of  $\Delta d$  on the whole wafer surface is defined as  $\Delta d_{max}$ , as shown in Fig. 10. The effects of  $e_{rd}$ ,  $e_{cd}$ ,  $e_{vd}$  and  $e_{wd}$  on GID were evaluated. The error distributions on the wafer surface were also plotted to help understand the way how the positioning errors affect the measurement results.

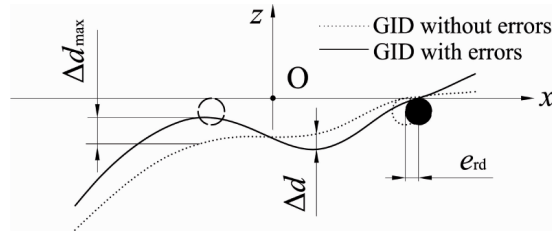


Fig. 10. The definitions of  $e_{rd}$ ,  $\Delta d$ , and  $\Delta d_{max}$ .

### 5.1. Effect of $e_{rd}$ on GID

There is a good linear relationship between  $\Delta d_{max}$  and  $e_{rd}$  of one supporting ball, as shown in Fig. 11, in which the positive and negative  $e_{rd}$  values mean the outward and inward shifts of the positioning ball, respectively.  $\Delta d_{max}$  changes about  $3 \mu\text{m}/\text{mm}$  for  $e_{rd}$  ( $11.7 \mu\text{m}$  in the positive direction and  $13.5 \mu\text{m}$  in the negative direction versus  $4 \text{ mm } e_{rd}$ ). To obtain the measurement accuracy of 1 micrometer or less on a wafer with diameter of 300 mm and thickness of  $400 \mu\text{m}$  with  $R_s$  being 98 mm,  $e_{rd}$  should be less than  $296 \mu\text{m}$ .

The distribution of  $\Delta d$  on the wafer surface caused by 1 mm  $e_{rd}$  remains axially symmetric, which is shown in Fig. 12.  $\Delta d_{max}$  occurs at the edge of the wafer near the deviated supporting ball.  $\Delta d$  is negative in the center, and positive at the edge of the wafer.

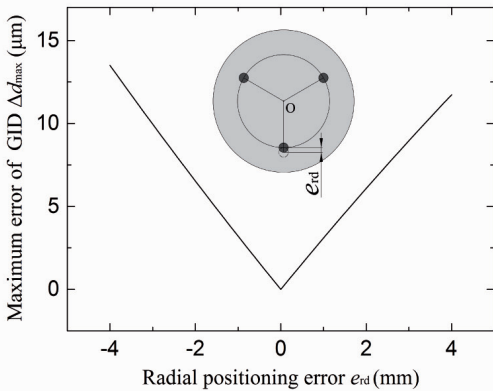


Fig. 11. The relation between  $\Delta d_{max}$  and  $e_{rd}$ .

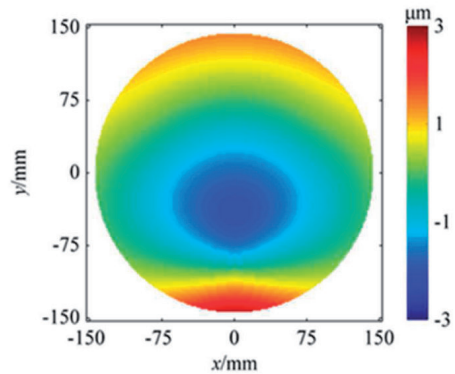


Fig. 12. The  $\Delta d$  distribution on the wafer surface caused by  $e_{rd}$  ( $e_{rd}=1 \text{ mm}$ ).

### 5.2. Effect of $e_{cd}$ on GID

Figure 13 demonstrates the effect of  $e_{cd}$  of one supporting ball on  $\Delta d_{max}$ .  $\Delta d_{max}$  changes about  $9 \mu\text{m}/\text{mm}$  for  $e_{cd}$  ( $34.4 \mu\text{m}$  versus  $4 \text{ mm } e_{cd}$ ). The effect of  $e_{cd}$  is much larger compared with that of  $e_{rd}$ . To obtain the measurement accuracy of 1 micrometer or less on a wafer with diameter of 300 mm and thickness of  $400 \mu\text{m}$  with  $R_s$  being 98 mm,  $e_{cd}$  should be less than  $116 \mu\text{m}$ .

The  $\Delta d$  distribution of the wafer caused by  $e_{cd}$  is not symmetric along the  $x$  axis, as shown in Fig. 14. However, its absolute value distribution exhibits an axial symmetry along the  $y$  axis. Larger difference values are on the half of the wafer where the supporting ball is deviated from the ideal position. The maximum positive difference value is located at the wafer edge where the circumferential position is at  $\theta = 45^\circ$  and the maximum negative difference is at  $\theta = -45^\circ$ . The difference value on the other half of the wafer is much smaller.

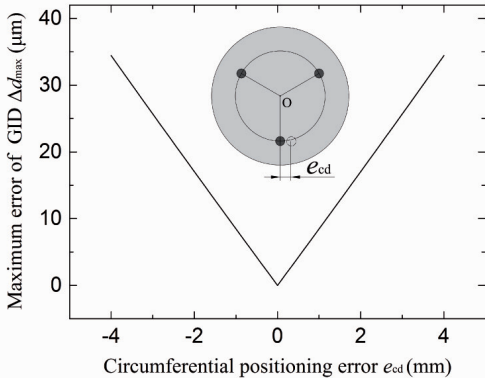


Fig. 13. The relation between  $\Delta d_{\max}$  and  $e_{cd}$ .

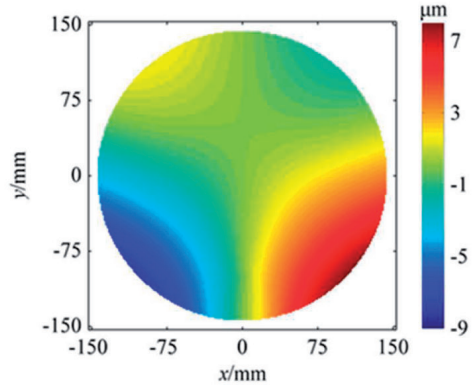


Fig. 14. The  $\Delta d$  distribution on the wafer surface caused by  $e_{cd}$  ( $e_{cd} = 1$  mm).

### 5.3. Effect of $e_{vd}$ on GID

A cosine type relationship between  $\Delta d_{\max}$  and  $e_{vd}$  is found, as shown in Fig. 15. The effect of the positive  $e_{vd}$  is a little larger than that of the negative one.  $\Delta d_{\max}$  changes less than 0.2  $\mu\text{m}$  when  $e_{vd}$  is equal to 4 mm. It is easy to achieve the positioning accuracy of the supports along the vertical direction. To obtain the measurement accuracy of 0.1 micrometer or less the effect of vertical positioning error  $e_{vd}$  is insignificant. It should be noted that the measurement range would increase if the supporting ball have an  $e_{vd}$  error, often leading to the decrease of measurement accuracy.

The  $\Delta d$  distribution on the wafer surface is shown in Fig. 16 when  $e_{vd}$  equals to 1 mm. Its topography caused by  $e_{vd}$  is quite similar to that caused by  $e_{cd}$  (Fig. 12). The reason is that the distance between the deviated supporting ball and the other two fixed balls increases when the supporting ball is incorrectly positioned in the vertical direction, leading to an error along the radial direction. It is also the reason of the relationship between  $\Delta d_{\max}$  and  $e_{vd}$  being a cosine type.

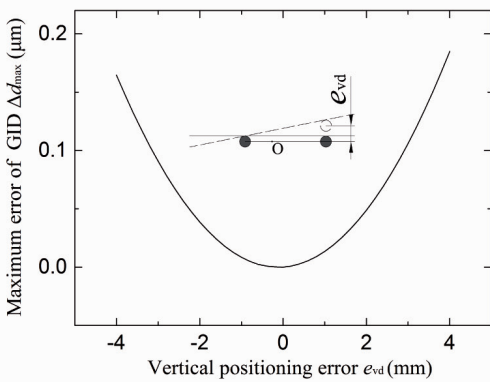


Fig. 15. The relation between  $\Delta d_{\max}$  and  $e_{vd}$ .

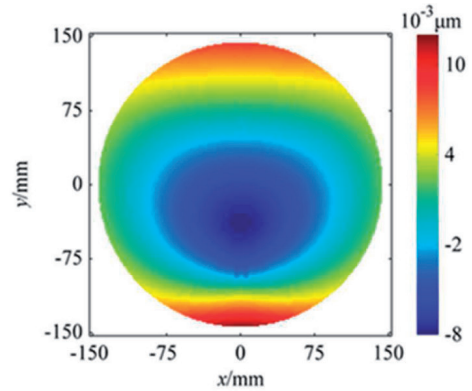


Fig. 16. The  $\Delta d$  distribution on the wafer surface caused by  $e_{vd}$  ( $e_{vd} = 1$  mm).

### 5.4. Effect of $e_{wd}$ on GID

It is extremely difficult or even impossible to have the wafer exactly concentric with the circle determined by three balls in the supporting mechanism. The effect of  $e_{wd}$  was investigated to provide a guideline in designing a centering device.

$\Delta d_{max}$  changes about  $8 \mu\text{m}/\text{mm}$  for  $e_{wd}$  ( $29.0 \mu\text{m}$  in the positive direction and  $33.1 \mu\text{m}$  in the negative direction versus  $4 \text{ mm } e_{wd}$ ), as shown in Fig. 17. There exist negative errors on the two sides where the supporting ball is deviated from the ideal position. As shown in Fig. 18, the maximum positive error is at the wafer edge at  $\theta = 180^\circ$  which is opposite to the deviated supporting ball. The maximum negative error is on the right or left wafer edge where the circumferential positions are at  $\theta = 90^\circ$  or at  $\theta = -90^\circ$ .

Figure 19 shows the effect of  $e_{wd}$  on  $\Delta d_{max}$  in three different angular directions.  $\Delta d_{max}$  is about  $35.1 \mu\text{m}$  along three different directions when the wafer center is burdened with a positioning error of  $4 \text{ mm}$ . The  $\Delta d_{max}$  differences of three directions are small compared with the maximum value. The effect of angular direction of  $e_{wd}$  is negligible. To obtain the measurement accuracy of  $1 \text{ micrometer}$  or less, the positioning error should be less than  $114 \mu\text{m}$  for the center positioning accuracy of the wafer.

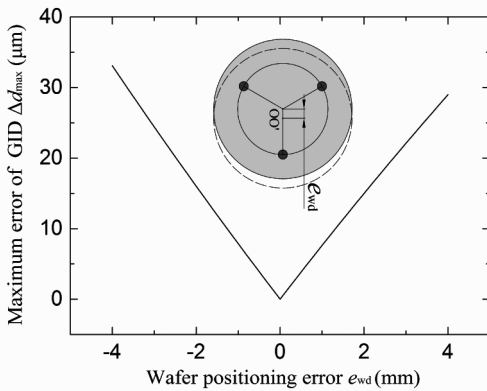


Fig. 17. The relation between  $\Delta d_{max}$  and  $e_{wd}$ .

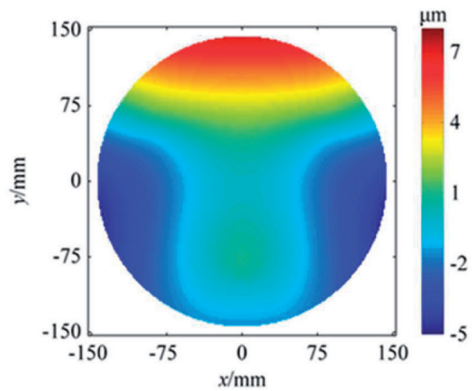


Fig. 18. The  $\Delta d$  distribution on the wafer surface caused by  $e_{wd}$  ( $e_{wd} = 1 \text{ mm}$ ).

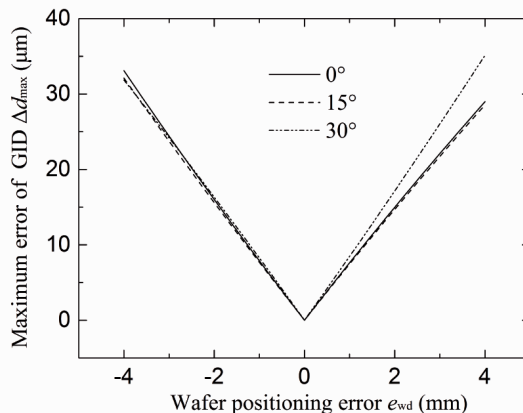


Fig. 19. The effect of  $e_{wd}$  in different directions on  $\Delta d_{max}$ .

## 6. Discussion

The GID is uniquely determined by the positions of the supports for a silicon wafer in the three-point-support method, which is a desired feature compared with other methods in which the wafer is placed on a work plane directly or supported at its peripheries during measurement.

The GID of the wafer could be subtracted from the measurement results to obtain the accurate unconstrained shape of the wafer. Compared with the inverting method, the proposed method is time-saving, since only one surface needs to be scanned, and the wafer is not required to be flipped during measurement. The wafer has to be flipped during measurement using the inverting method as both surfaces have to be measured. An accurate FEM of the wafer is essential because it influences the final result directly in the three-point-support method.

The difference between the GIDs considering initial stress and without considering initial stress is over 10  $\mu\text{m}$ , indicating that the effect of the initial stress has to be taken into consideration for wafers after grinding or lapping. Theoretically, the effect of the initial stress on GID calculation could be considered in the FEM. The results of this study show that for wafers with a uniform subsurface damage layer, *i.e.* initial stress distribution, the true shape and the GID of wafer could be obtained through iterative calculations with the aid of the Stoney equation, even though the actual depth of the subsurface damage and the initial stress value are unknown. For wafers with non-uniform initial stress distribution, the initial stress could also be applied according to the stress distribution on the wafer surface [24] as the applying of the initial stress is element-based in the FEM. It can be seen from Fig. 6 that the difference of GIDs between the wafer surface under the initial stress being in upward and downward positions could be identified by our FEM. Although it is difficult to directly verify the FEM at this moment, the proposed method provides a potential way for the flatness measurement of large and thin wafers considering the effect of the initial stress.

The three-point-support method is based on the concept of superposition of multiple deflections. The bifurcation will occur if the wafer thickness is too small for the proposed method to be used. Therefore, the minimum wafer thickness that can be tolerated should be the critical thickness, at which the bifurcation does not occur on the wafer. The criterion for checking whether the bifurcation occurs has been discussed in the previous work [25]. It can be expressed as a function of the diameter, the thickness and the initial stress:

$$A = (\sigma t) \frac{D^2}{h^3}, \quad (2)$$

where:  $A$  is the criterion value: if  $A > A_c$ , the bifurcation will occur;  $(\sigma t)$  is the force per unit width, which is related to the wafer surface quality, and can be derived from the surface deformation;  $D$  is the wafer diameter; and  $h$  – the wafer thickness. The minimal thickness can then be obtained by substituting  $A_c$ ,  $D$  and  $(\sigma t)$  into the equation. The critical value is  $A_c = 680 \text{ GPa}$  for silicon. For wafers after grinding with #5000 diamond wheel,  $(\sigma t)$  is about  $0.15 \text{ GPa} \cdot \mu\text{m}$ . The minimum thicknesses of wafers with diameters of 200 mm and 300 mm were calculated to be 207  $\mu\text{m}$  and 271  $\mu\text{m}$ , respectively. For wafers after polishing or etching, the surface quality is much better than for those after grinding, of which the force per unit width is much smaller, resulting in smaller minimum wafer thickness values.

Positioning errors of the supporting mechanism are introduced during the manufacturing and assembling processes, leading to measurement errors. In this paper the effects of positioning errors of supports were studied to determine the accuracy requirements for a supporting mechanism. The effect of the positioning error of the wafer was also studied

and it is used to determine the accuracy requirement of a centering device for the wafer. To obtain the measurement accuracy of 1 micrometer on wafers with 300 mm diameter and 400  $\mu\text{m}$  thickness, the positioning errors should be less than 296  $\mu\text{m}$  in the radial direction, 116  $\mu\text{m}$  in the circumferential direction for the supporting balls, and 114  $\mu\text{m}$  for the center positioning accuracy of the wafer. It should be noted that the required positioning accuracy and the centering accuracy are both over 100  $\mu\text{m}$ , which is not difficult to achieve in the production environment.

On the other hand, the positions of supporting balls could be obtained by measuring their profiles. The supporting points are the highest points of the balls. The position of the wafer could also be obtained by measuring its edges. The center of the silicon wafer could be calculated after knowing the positions of over three its edge points. Then, the positions of the supporting balls and the wafer are the feedback to the FEM and the agreement of positions of supports and wafer in both the measuring experiment and the FEM could be attained. In this way, it is not necessary to require a high positioning accuracy any more.

The three-point-support method is feasible as a verification method for a single wafer. However, its use in a production environment may be limited because both the FEM calculation and the profile scanning by laser sensor need time.

## 7. Conclusions

An FEM which included the effect of initial stress was developed to calculate the GID of silicon wafers. The simulated GID of a double-sided polished wafer agreed well with that of the measured one. For wafers with 300 mm diameter and 400  $\mu\text{m}$  thickness of which the PV value caused by the initial stress was 300  $\mu\text{m}$ , the maximum difference value between GIDs with and without considering the initial stress was over 10  $\mu\text{m}$  while the GID range without considering the initial stress was 147.1  $\mu\text{m}$ . The maximum difference value between GIDs of a silicon wafer before and after the flip of the wafer reached 9.8  $\mu\text{m}$ . The measurement result of a silicon wafer ground with #5000 diamond grinding wheel was consistent with the simulation result, both demonstrating that the effect of initial stress could not be neglected in the FEM.

The effects of the positioning errors of the supporting balls and the wafer were investigated. Different patterns of error distributions were found for different types of errors. The effect of the vertical positioning error was negligible. To obtain the measurement accuracy of 1 micrometer on 300 mm diameter, 400  $\mu\text{m}$  thickness wafers, the positioning errors should not exceed 296  $\mu\text{m}$  in the radial direction, 116  $\mu\text{m}$  in the circumferential direction for the supporting balls, and 114  $\mu\text{m}$  for the center positioning accuracy of the wafer. The study results show that the wafer positioning error and the circumferential error are the most influential factors affecting the measurement accuracy. For 300 mm diameter wafers with thickness larger than 400  $\mu\text{m}$  the accuracy requirement becomes less strict. Similarly, for 400  $\mu\text{m}$  thickness wafers with diameter smaller than 300 mm the effect of the errors of the supports is smaller.

## Acknowledgments

The authors would like to acknowledge the financial support from the National Natural Science Foundation of China (91323302), Science Fund for Creative Research Groups of NSFC (51321004), the State Key Development Program for Basic Research of China (2011CB013201), the National High Technology Research and Development Program of China (2013AA040104) and National Science and Technology Major Project of China (2014ZX02504001). We are very grateful for the discussion with Professor Bi Zhang.

## References

- [1] Burghartz, J.N., Appel, W., Harendt, C., Rempp, H., Richter, H., Zimmermann, M. (2009). Ultra-thin chips and related applications, a new paradigm in silicon technology. *ESSCIRC 2009. Proc. of the 35th European Solid-State Circuits Conference*, Athens, Greece, 28–35.
- [2] Gurnett, K., Adams, T. (2006). Ultra-thin semiconductor wafer applications and processes. *III-Vs Review*, 19(4), 38–40.
- [3] Kim, Y.S., Maeda, *et al.* (2013). Advanced wafer thinning technology and feasibility test for 3D integration. *Microelectronic Engineering*, 107, 65–71.
- [4] Fei, G., Xiaoyun, D., Gaowei, X., Le, L. (2009). A wafer-level 3D packaging structure with Benzocyclobutene as a dielectric for multichip module fabrication. *Journal of Semiconductors*, 30(10), 106003.
- [5] Draney, N.R., Liu, J.J., Jiang, T. (2004). Experimental investigation of bare silicon wafer warp. *IEEE Workshop on Microelectronics and Electron Devices, WMED: IEEE Electron Devices Northwest Regional Meeting*, Boise, ID, United states, 120–123.
- [6] Ng, C.S., Asundi, A.K. (2011). Warpage measurement of thin wafers by reflectometry. *Physics Procedia*, 19, 9–20.
- [7] SEMI. (2007). Test method for measuring bow and warp on silicon wafers by automated noncontact scanning. <http://www.semi.org>
- [8] Gao, S., Dong, Z., Kang, R., Zhang, B., Guo, D. (2015). Warping of silicon wafers subjected to back-grinding process. *Precision Engineering*, 40, 87–93.
- [9] Chu, J., Griesmann, U., Wang, Q., Soons, J.A., Benck, E.C. (2010). Deformation-free form error measurement of thin, plane-parallel optics floated on a heavy liquid. *Applied Optics*, 49(10), 1849–1858.
- [10] Griesmann, U., Wang, Q., Benck, E.C., Chu, J., Sohn, J. (2010). Flatness measurements of thin, plane-parallel optics floated on a heavy liquid. *ASPE 2010 Summer Topical Meeting on Precision Interferometric Metrology*, Ashville, NC, 62–66.
- [11] Natsu, W., Ito, Y., Kunieda, M., Naoi, K., Iguchi, N. (2005). Effects of support method and mechanical property of 300 mm silicon wafer on sori measurement. *Precision Engineering*, 29(1), 19–26.
- [12] Ito, Y., Natsu, W., Kunieda, M., Maruya, N., Iguchi, N. (2006). Accuracy estimation of shape measurement of thin-large panel with three-point-support inverting method. *JSME International Journal, Series C: Mechanical Systems, Machine Elements and Manufacturing*, 49(3), 930–934.
- [13] Shams, M., Destrade, M., Ogden, R.W. (2011). Initial stresses in elastic solids: Constitutive laws and acoustoelasticity. *Wave Motion*, 48(7), 552–567.
- [14] Zarudi, I., *et al.* (1996). Subsurface damage in single-crystal silicon due to grinding and polishing. *Journal of Materials Science Letters*, 15(7), 586–587.
- [15] Yukihiro, I., Wataru, N., Masanori, K. (2010). Effect of Anisotropy on Shape Measurement Accuracy of Silicon Wafer Using Three-Point-Support Inverting Method. *Journal of Advanced Mechanical Design, Systems, and Manufacturing*, 4(5), 1066–1075.
- [16] Hopcroft, M.A., Nix, W.D., Kenny, T.W. (2010). What is the Young's Modulus of Silicon? *Journal of Microelectromechanical Systems*, 19(2), 229–238.
- [17] Boryczko, A., Rytlewski, W. (2014). Surface irregularities as a complex signal of tool representation together with uneven displacement in respect to the workpiece. *Metrol. Meas. Syst.*, 21(1), 133–144.
- [18] Iwasinska-Kowalska, O. (2014). A system for precise laser beam angular steering. *Metrol. Meas. Syst.*, 21(1), 27–36.
- [19] Huang, H., Wang, B.L., Wang, Y., Zou, J., Zhou, L. (2008). Characteristics of silicon substrates fabricated using nanogrinding and chemo-mechanical-grinding. *Materials Science and Engineering: A*, 479(1–2), 373–379.
- [20] Zhang, P.F., Pei, Z.J. (2009). Lapping of semiconductor wafers: An experimental investigation on subsurface damage. *Proc. of the ASME International Manufacturing Science and Engineering Conference 2009, MSEC2009*, West Lafayette, IN, United States, 715–719.
- [21] Wang, Y., Zou, J., Huang, H., Zhou, L., Wang, B.L., Wu, Y.Q. (2007). Formation mechanism of nanocrystalline high-pressure phases in silicon during nanogrinding. *Nanotechnology*, 18(46), 465705.

- [22] Wu, Y.Q., Huang, H., Zou, J., Zhang, L.C., Dell, J.M. (2010). Nanoscratch-induced phase transformation of monocrystalline Si. *Scripta Materialia*, 63(8), 847–850.
- [23] Huang, H., Wu, Y.Q., Wang, Y., Zou, J., Zhou, L. (2009). Subsurface structures of monocrystalline silicon generated by nanogrinding. *Key Engineering Materials*, 389–390, 465–468.
- [24] Gao, S., Kang, R., Dong, Z., Guo, D. (2013). Subsurface damage distribution in silicon wafers ground with wafer rotation grinding method. *Jixie Gongcheng Xuebao/Journal of Mechanical Engineering*, 49(3), 88–94.
- [25] Janssen, G.C.A.M., Abdalla, M.M., van Keulen, F., Pujada, B.R., van Venrooy, B. (2009). Celebrating the 100th anniversary of the Stoney equation for film stress: Developments from polycrystalline steel strips to single crystal silicon wafers. *Thin Solid Films*, 517(6), 1858–1867.
- [26] Feng, X., Huang, Y., Rosakis, A.J. (2007). On the Stoney Formula for a Thin Film/Substrate System With Nonuniform Substrate Thickness. *Journal of Applied Mechanics*, 74(6), 1276.